

Analysis of phase regeneration of DPSK/DQPSK signals based on phase-sensitive amplification

Xianfeng Tang (唐先锋)^{1,2*}, Xiaoguang Zhang (张晓光)^{1,2}, and Lixia Xi (席丽霞)^{1,2}

¹*Institute of Optical Communication and Optoelectronics, Beijing University of Posts and Telecommunications, Beijing 100876, China*

²*Key Laboratory of Optical Communication and Lightwave Technologies, Ministry of Education, Beijing University of Posts and Telecommunications, Beijing 100876, China*

*E-mail: txf2110@hotmail.com

Received July 8, 2008

Amplification and phase regeneration can be realized using a phase-sensitive amplifier (PSA). The phase regeneration of differential phase-shift keying (DPSK) signals based on PSA is analyzed theoretically. We realize the phase regeneration of differential quadrature phase-shift keying (DQPSK) signals based on a structure using two balanced PSAs. Simulations show that nearly ideal phase regeneration can be achieved for the DPSK/DQPSK signals.

OCIS codes: 060.2330, 060.2340, 060.2360, 060.4510.

doi: 10.3788/COL20090705.0380.

Differential phase-shift keying (DPSK) and differential quadrature phase-shift keying (DQPSK) have received renewed attention recently for long-haul transmission or spectrally efficiency systems, due to the improvement in receiver sensitivity compared to on-off keying (OOK) and the enhanced tolerance to dispersion and nonlinear effects, particularly intrachannel four-wave mixing (FWM). Excluding timing jitter, the primary limitation of a DPSK/DQPSK transmission system is the accumulation of linear and nonlinear phase noises. Experiments have shown that when the nonlinear contribution to phase noise becomes dominant, the improvement in receiver sensitivity for balanced DPSK detection can be lost^[1]. Many schemes have been proposed, including mid-link spectral inversion^[2], post nonlinear phase-shift compensators^[3], and phase-preserving amplitude regeneration^[4]. But they are rather difficult to realize or have not been demonstrated experimentally. Phase-sensitive amplifier (PSA) has been demonstrated to have the ability of both amplifying the signals and simultaneously achieving phase regeneration^[5,6]. In this letter, at first we analyze analytically and numerically the phase regeneration of DPSK signals based on PSA. Then we design a structure for the phase regeneration of DQPSK signals using two balanced PSAs.

Nonlinear Mach-Zehnder interferometers (MZIs), when

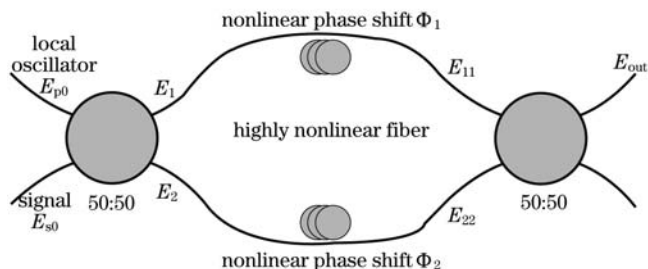


Fig. 1. Structure of PSA.

driven by a phase-locked local oscillator pump, can provide phase-sensitive amplification to input signals. The phase-sensitive nature of the optical gain forces the signal (degraded data) phase to a value of 0 or π relative to the strong pump at the same frequency. Regeneration is then realized. The structure of such a PSA is shown in Fig. 1.

In the structure, two highly nonlinear fibers (HNLFs) of equal electric susceptibility and length are introduced into two arms of the MZI and the device becomes a nonlinear MZI. The pump E_{p0} and signal E_{s0} are combined in the input coupler into the nonlinear MZI, and the outputs of the input coupler is given by

$$E_1 = \frac{1}{\sqrt{2}}(jE_{p0} + E_{s0}), \quad (1)$$

$$E_2 = \frac{1}{\sqrt{2}}(E_{p0} + jE_{s0}). \quad (2)$$

Due to the different powers of E_1 and E_2 , the phase shifts in the HNLFs are different too, labelled as Φ_1 and Φ_2 for the top and bottom arms of the MZI, respectively. The nonlinear phase shifts through both arms of the MZI are given by

$$\begin{aligned} \Phi_1 &= \gamma L \left(\frac{(jE_{p0} + E_{s0})(-jE_{p0}^* + E_{s0}^*)}{\sqrt{2}\sqrt{2}} \right) \\ &= \frac{\gamma L}{2} (|E_{p0}|^2 + |E_{s0}|^2) + \gamma L |E_{p0}| |E_{s0}| \sin(\delta) \\ &= \Phi_0 + \Phi_{nl}, \end{aligned} \quad (3)$$

$$\begin{aligned} \Phi_2 &= \gamma L \left(\frac{(E_{p0} + jE_{s0})(E_{p0}^* - jE_{s0}^*)}{\sqrt{2}\sqrt{2}} \right) \\ &= \frac{\gamma L}{2} (|E_{p0}|^2 + |E_{s0}|^2) - \gamma L |E_{p0}| |E_{s0}| \sin(\delta) \\ &= \Phi_0 - \Phi_{nl}, \end{aligned} \quad (4)$$

where γ is the fiber nonlinear coefficient, L is the amplifier length, $\Phi_0 = (\gamma L/2)(|E_{p0}|^2 + |E_{s0}|^2)$, $\Phi_{nl} = \gamma L |E_{p0}| |E_{s0}| \sin(\delta)$ is the nonlinear phase shift, $\delta = \Phi_{s0} - \Phi_{p0}$ is the relative signal-pump phase, Φ_{s0} and Φ_{p0} are the signal and pump phases. So E_{11} and E_{22} can be written as

$$E_{11} = \frac{e^{j\Phi_1}}{\sqrt{2}}(jE_{p0} + E_{s0}), \quad (5)$$

$$E_{22} = \frac{e^{j\Phi_1}}{\sqrt{2}}(E_{p0} + jE_{s0}). \quad (6)$$

The output at the signal port is given by

$$E_{out} = e^{j\Phi_0}(-jE_{p0}\sin\Phi_{nl} + jE_{s0}\cos\Phi_{nl}). \quad (7)$$

From the above equation, it follows that the output signal peak power P_{out} is given by

$$P_{out} = P_{s0}\cos^2\Phi_{nl} + P_{p0}\sin^2\Phi_{nl} - \sqrt{P_{s0}P_{p0}}\sin(2\Phi_{nl})\cos\delta. \quad (8)$$

From Eqs. (7) and (8), it is shown that the coupling between the pump and signal is phase sensitive. When $\delta = \pm \pi/2$, the nonlinear phase shift Φ_{nl} reaches the maximum value; when $\delta = 0$ or π , the nonlinear phase shift Φ_{nl} vanishes and there will be no coupling between the pump and signal. The signal gain is determined by the nonlinear phase shift Φ_{nl} : when the nonlinear phase shift is 0, the signal output power is equal to the input signal power, so there is no energy transferred from the pump to the signal port; when the nonlinear phase shift is $\pi/2$, the signal output power is equal to the input pump power.

Figure 2 shows the phasor diagram of the normalized field gain, defined as $|E_{out}|/|E_{s0}|$, as a function of the relative signal-pump phase. From the figure, it is clear that, when the input signals have the relative phase of approximate multiples of $\pi/2$, the field components are amplified strongly, with the gain of around 3.5; while those with the relative phase near the integers of π to the pump are not amplified, with a gain of nearly 0.

Setting the phase of the pump to be $\pi/2$, the input

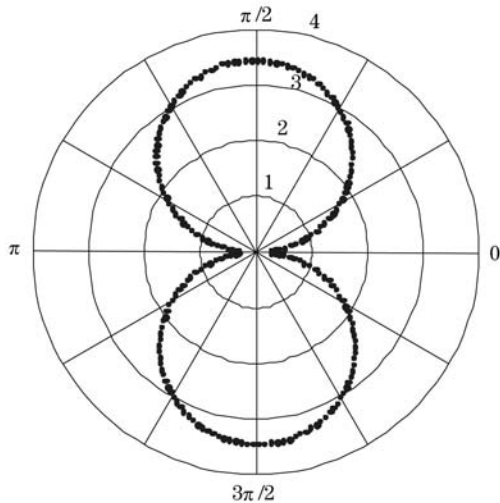


Fig. 2. Phasor diagram of normalized field gain.

signals that have the phase of near 0 and π are amplified strongly; while the noises that have the phase of near $\pi/2$ and $3\pi/2$ are nearly eliminated. Then the output phase of the signal is forced to a nearly constant value for large variations of input signal phase. The difference between the two output phase states is verified to be exactly π . Then regeneration is realized.

The DQPSK phase regenerator is composed of 2 PSAs. Figure 3 is the scheme for DQPSK signals. In the scheme, two PSAs with different pumps are introduced into the two arms of a symmetric fiber MZI. The degraded signals are split into two sections through a 50:50 splitter which are regenerated in the top and bottom arms respectively. E_{s1} and E_{s2} are given by

$$E_{s1} = \frac{1}{\sqrt{2}}jE_s, \quad (9)$$

$$E_{s2} = \frac{1}{\sqrt{2}}E_s. \quad (10)$$

Here we adopt the optical phase distribution of 0, $\pi/2$, π , $3\pi/2$ for DQPSK signals. In the top PSA, the phase of pump1 is set to be $\pi/2$, so it can regenerate symbols having the phases of 0 and π . In the bottom PSA, the phase of pump2 is shifted by $\pi/2$ relative to pump1, so it can regenerate symbols having the phases of $\pi/2$ and $3\pi/2$. E_{out1} and E_{out2} can be described as

$$E_{out1} = e^{j\Phi_0}(-jE_{p1}\sin\Phi_{nl1} + jE_{s1}\cos\Phi_{nl1}), \quad (11)$$

$$E_{out2} = e^{j\Phi_0}(-jE_{p2}\sin\Phi_{nl2} + jE_{s2}\cos\Phi_{nl2}), \quad (12)$$

where $E_{p2} = -jE_{p1}$, $\Phi_0 = \gamma L/2(|E_{p1}|^2 + |E_{s1}|^2) = \gamma L/2(|E_{p2}|^2 + |E_{s2}|^2)$, $\Phi_{nl1} = \gamma L |E_{p1}| |E_{s1}| \sin(\delta_1)$ is the top nonlinear phase shift, $\delta_1 = \Phi_{s1} - \Phi_{p1}$ is the top relative signal-pump phase, $\Phi_{nl2} = \gamma L |E_{p2}| |E_{s2}| \sin(\delta_2)$ is the bottom nonlinear phase shift, $\delta_2 = \Phi_{s2} - \Phi_{p2}$ is the bottom relative signal-pump phase.

At the output coupler, the two regenerated signals are recombined to form the regenerated DQPSK signal as

$$\begin{aligned} E_{out} &= \frac{j}{\sqrt{2}}E_{out1} + \frac{1}{\sqrt{2}}E_{out2} \\ &= \frac{1}{\sqrt{2}}e^{j\Phi_0}(E_{p1}(\sin\Phi_{nl1} - \sin\Phi_{nl2}) \\ &\quad - jE_s(\cos\Phi_{nl2} - \cos\Phi_{nl1})). \end{aligned} \quad (13)$$

Simulations are carried out based on the principle discussed above. The pump and signal input powers are 20 mW and 175 μ W, respectively. The amplifier length is 6 km and $\gamma = 27 \text{ W}^{-1}\text{km}^{-1}$. Uniformly distributed noises of amplitude and phase are added. Balanced detection is used to demodulate both DPSK and DQPSK signals.

Now we consider the simulation of phase regeneration of DPSK signals. We define $I_{diff} = |E_{out1}|^2 - |E_{out2}|^2$. When there is no noise of amplitude, $I_{diff} = \cos(\Phi_n - \Phi_{n-1})$, where $\Phi_n - \Phi_{n-1}$ is the phase difference between the current bit of data and the subsequent bit. For signals without noises of amplitude and phase, the value is either +1 or -1. When noises are added, the values will be around ± 1 , and the values around 0 will cause bit error.

Figures 4 and 5 show the polar graphs of the data and histogram of 10000 received data (I_{diff}) before and

after regeneration. From Fig. 4, we can see that the total phase variation is nearly $\pi/2$ before regeneration; however, after regeneration, the phase noise is greatly reduced and the output phase states have a difference of

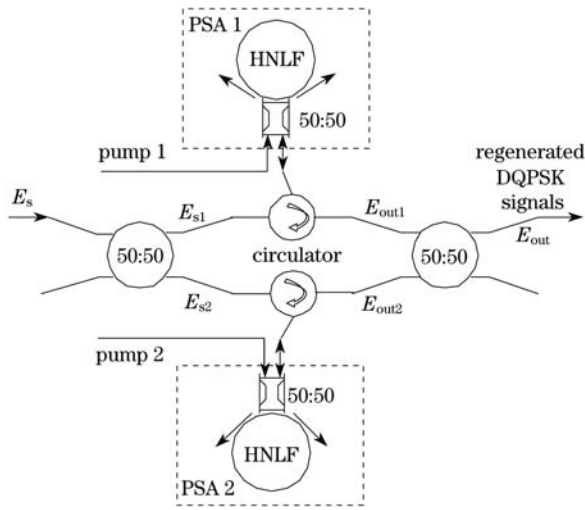


Fig. 3. PSA scheme for DQPSK signals.

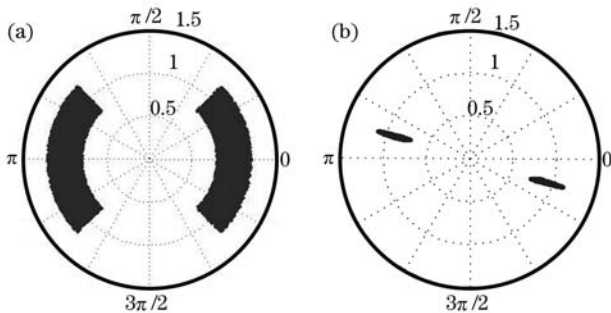


Fig. 4. Phase distributions (a) before regeneration (E_{s0}) and (b) after regeneration (E_{out}) of DPSK signals.

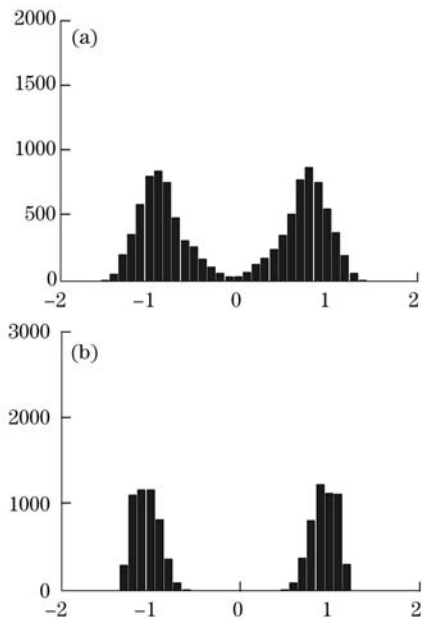


Fig. 5. Received data I_{diff} (a) before and (b) after regeneration of DPSK signals.

π . From Fig. 5, the received data that have the values around 0 causing bit error are also greatly reduced, so it is easier to determine “0” and “1” bits from I_{diff} around ± 1 . Then regeneration is realized. The improvement of bit error rate (BER) is shown in Fig. 6, in which OSNR means optical signal-to-noise ratio.

Now we consider the simulation of phase regeneration of DQPSK signals. Figure 7 shows the phase distributions of DQPSK data in the process of regeneration. Figures 8 and 9 show histograms of 10000 received data (I_{diff}) of the u port and v port of the balanced detector. From Fig. 7, we can see that the total phase variation is nearly $\pi/3$ before regeneration; however, after the two PSAs, the phase noise is greatly reduced and the output phase states of each arm have a difference of π ; the recombined DQPSK data have four phase states with a difference of $\pi/2$. From Figs. 8 and 9, the received data that have the values around 0 causing bit error are also greatly reduced, so it is easier to determine “0” and “1” bits from I_{diff} around ± 1 . Then we can see that nearly ideal phase regeneration of DQPSK signal is realized.

In conclusion, we have analyzed the phase regeneration of DPSK signals. A scheme of phase regeneration of DQPSK signals is analyzed theoretically. Simulation shows that nearly ideal regeneration is realized. The

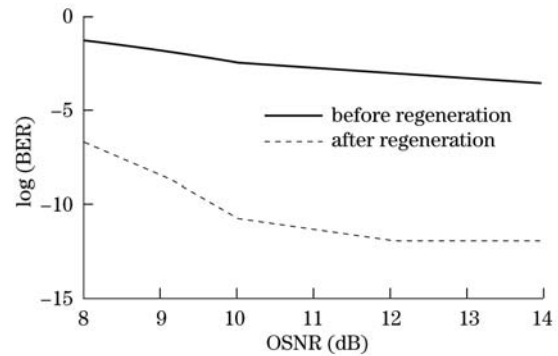


Fig. 6. BER before and after regeneration.

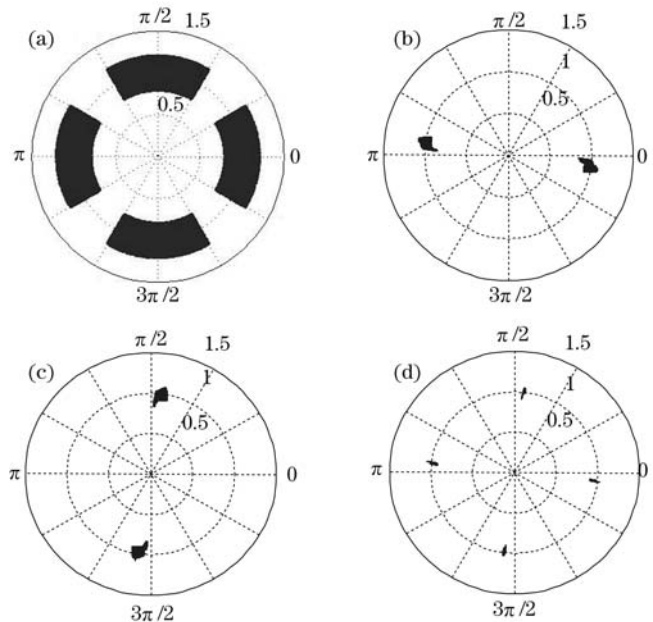


Fig. 7. Phasor diagram of DQPSK data (a) before regeneration (E_s), (b) after the first PSA (E_{out1}), (c) after the second PSA (E_{out2}), (d) after regeneration (E_{out}).

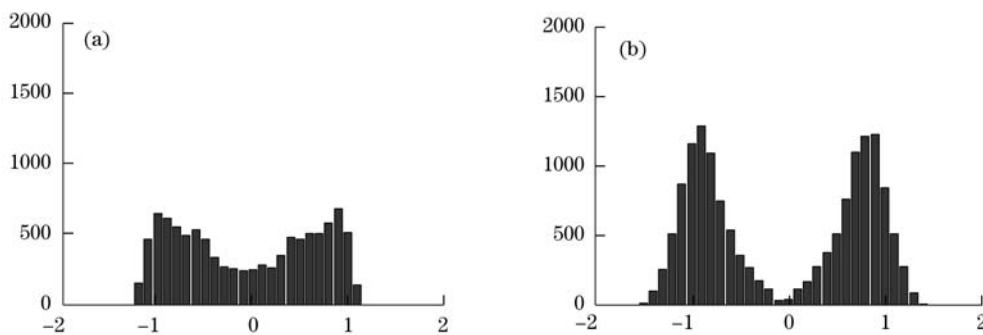


Fig. 8. Received data in u port (a) before and (b) after regeneration of DQPSK signals.

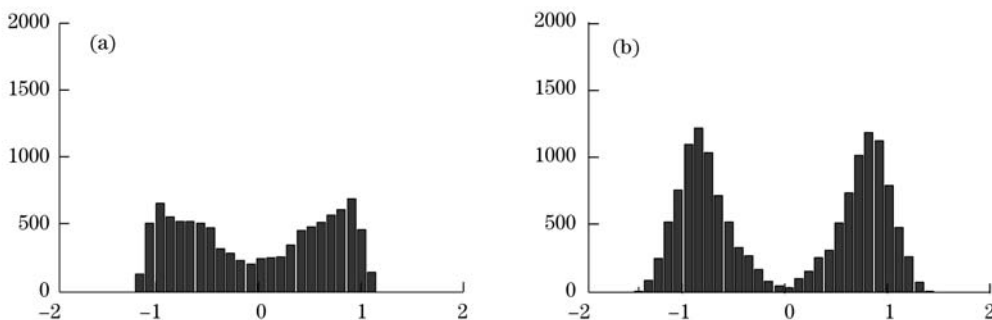


Fig. 9. Received data in v port (a) before and (b) after regeneration of DQPSK signals.

BER improvement is slightly greater than two orders of magnitude. And further BER improvement can be obtained by phase-and-amplitude regeneration based on PSA in the depleted-pump regime. In the simulation, the length of the amplifier is a little long, however, if we adopt novel photonic crystal^[7] or bismuth-oxide-based HNLF with a higher fiber nonlinear coefficient, the length will be greatly reduced^[8].

This work was supported by the Beijing Education Committee Common Build Foundation (No. XK100130637) and the National “863” Program of China (No. 2009AA01Z224).

References

1. H. Kim and A. H. Gnauck, *IEEE Photon. Technol. Lett.* **15**, 320 (2003).
2. S. L. Jansen, D. van den Borne, G. D. Khoe, H. de Waardt, C. C. Monsalve, S. Spälter, and P. M. Krummrich, in *Proceedings of OFC 2005* OTh05 (2005).
3. C. Xu and X. Liu, *Opt. Lett.* **27**, 1619 (2002).
4. A. Striegler and B. Schmauss, *IEEE Photon. Technol. Lett.* **16**, 1083 (2004).
5. K. Croussore, C. Kim, and G. Li, *Opt. Lett.* **29**, 2357 (2004).
6. K. Croussore, I. Kim, Y. Han, C. Kim, and G. Li, *Opt. Express* **13**, 3945 (2005).
7. F. Zhang, X. Liu, M. Zhang, and P. Ye, *Chin. Opt. Lett.* **5**, 260 (2007).
8. Y. Wei, X. Zhang, Y. Xu, Y. Huang, and X. Ren, *Acta Opt. Sin.* (in Chinese) **27**, 414 (2007).